Available online at www.sciencedirect.com
SCIENCE DIRECT®
Carbohydrate Research 340 (2005) 907–920
Carbohydrate RESEARCH

# Towards understanding the interaction between oligosaccharides and water molecules☆

Andrew Almond*

*Department of Biochemistry, University of Oxford, South Parks Road, Oxford OX1 3QU, United Kingdom*

Received 13 September 2004; accepted 10 January 2005

Dedicated to Professor David A. Brant

**Abstract**—Complex carbohydrates are implicated in many important biological processes, and have a strong interaction with water. This close interplay with molecular water through multiple hydroxyls may be an integral part of their emergent structure and dynamics, as selected during evolution. Using molecular dynamics simulations with explicit water the interactions at the linkages within a variety of oligosaccharides are investigated and contrasted, in order to establish correlations between linkage orientation, sugar epimerization, and water interaction. In particular, interactions at α linkages, and between mannose and glucose residues, that are common in oligosaccharides are considered. Sugars joined by α linkages at the 2-, 3-, and 6-position were found to interact via a combination of weak hydrogen-bonds and water-bridges, which is dependent on the epimerization state of the sugars. Due to their three-dimensional structure, they are also likely to interact with noncontiguous sugar residues in an oligosaccharide, which can lead to ordered structures through the exclusion of water. On the other hand, β linkages (to 3- and 4-position) maintain strong hydrogen-bonds, have a limited ability to be involved in water-bridges, and predominantly interact with the directly attached sugars. Therefore, sequences of α-linked sugars form compact, branched structures that have conformational flexibility, and β linkages form extended, relatively rigid structures, suitable for structural molecules, and at the termini of protein bound oligosaccharides. These results provide further tentative ties between chemical structure, water interactions, and the emergent form and function of specific sugars and linkages in oligosaccharides.


*Keywords:* Molecular dynamics; Oligosaccharide; Mannose; Conformation; Water

## 1. Introduction

Complex carbohydrates are integral components of the mammalian extracellular matrix. They are not usually found free, but are conjugated to other molecules to form glycoproteins, glycolipids, and proteoglycans. Although they are synthesized in the cell, their functions are almost exclusively restricted to the outside of the cell, either at the outer cell surface, or in the extracellular space. Unlike DNA and proteins, the biological roles of carbohydrates are not easy to define.[1] It has been postulated that they are involved in multivalent signaling processes, provide a way of identifying self, and a method of modulating the function and physical properties of proteins without modifying the genome. What is clear, though, is that complex carbohydrates are fundamental to many important biological processes including fertilization, immune defense, viral replication, parasitic infection, cell growth, cell–cell adhesion, degradation of blood clots, and inflammation.[2] From a physical point of view oligosaccharides occupy large volumes for their molecular weight, and vastly more so than globular proteins. This is exacerbated by their dynamic flexibility and ability to form branched structures. Therefore, even small oligosaccharides may shield and modify relatively large portions of the surfaces that they are attached to.

As is the case for all biological molecules, the three-dimensional structure of oligosaccharides partly dictates

☆ Submitted as part of a special issue recognizing the contributions of Professor David A. Brant to the field of carbohydrate research.

* Tel.: +44 1865 285332; fax: +44 1865 275253; e-mail: andrew.almond@bioch.ox.ac.uk

0008-6215/$ - see front matter © 2005 Elsevier Ltd. All rights reserved.
doi:10.1016/j.carres.2005.01.014

their interactions with other molecules.[3] Although the experimental analysis of carbohydrate three-dimensional structure can potentially improve the understanding of oligosaccharide function, it is fraught with difficulties; the majority resist crystallization and their NMR spectra are highly overlapped and frequently contain second-order line-shapes.[4] It is therefore necessary to use theoretical techniques to augment and help interpret the experimental data that can be gathered. However, there are complications in using theoretical approaches because oligosaccharides, unlike many proteins, are not thought to form ordered structures and their dynamic structures are highly dependent on interactions with water.[5] The close proximity of many hydroxyl moieties suggests that the molecular properties of water is central to an understanding of their structure and dynamics—rather than a mean-field approximation to water, such as inclusion of an enhanced dielectric. In some cases, the first shell water molecules may form integral parts of the dynamic conformation, and it is likely that the linkages and epimerization of sugars have been selected to take advantage of this interaction with water. Currently, however, little is known about these interactions. Molecular dynamics approaches using molecular mechanics force-fields are suitable for performing simulations of carbohydrates with inclusion of explicit water molecules, from which suitable analysis can extract the important water interactions.

Previous studies have used molecular dynamics techniques to investigate how water interacts with the surface of carbohydrates.[5–11] These simulations have underlined how the presence of molecular water influences the conformational population at carbohydrate linkages and therefore overall structure and dynamics. However, few studies have compared and contrasted water interactions across a variety of linkages and environments found in oligosaccharides. It is therefore uncertain as to whether conclusions made for individual linkages have any general basis. Previously we analyzed water structure, and compared the linkage dynamics, of oligosaccharides extracted from polysaccharides using molecular dynamics.[12] It was found, particularly at β-(1→4) linkages, that hydrogen-bond and water interactions could be correlated to dynamic behavior. However, no α-linkages, often found in oligosaccharides from glycoproteins, were considered in that analysis.

Recently we have performed molecular dynamics simulations of the oligosaccharides shown in Figure 1, using the TIP3P explicit water model. Simulations of oligosaccharides **1**, **2**, and **4** have been published previously;[13–15] the others have not. Also, simulations of oligosaccharides **1**, **2**, **4**, **5**, and **6** have been subjected to extensive experimental testing against NMR (NOESY cross-peaks, scalar, and residual dipolar couplings), X-ray fiber diffraction, and hydrodynamic data.[13–18] These molecular dynamics simulations, using explicit water,

Manα1→3Manα1→3Manα1→2Manα **(1)**

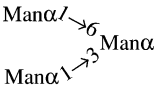

**(2)**

Glcα1→2Glcα1→3Glcα1→3Manα **(3)**

Fucα1→2Galβ1→4Glcβ **(4)**

GlcAβ1→3GlcNAcβ1→4GlcAβ1→3GlcNAcβ **(5)**

GlcAβ1→3GalNAcβ1→4GlcAβ1→3GalNAcβ **(6)**

**Figure 1.** Schematic showing the monosaccharide composition and the linkage geometry of the oligosaccharides considered in this article.

were found to be largely in agreement with the demanding experiments, which suggests that the simulations are not only providing realistic models of oligosaccharide conformation and dynamics, but also of the microscopic interactions with water.

By analysis of aqueous molecular dynamics simulations, the hydrogen-bonding dynamics and water structure at the linkages of oligosaccharides listed in Figure 1 are investigated, and then compared and contrasted. The analyzed structures contain a wide variety of sugar residues, linear and branched chains, and both α and β linkages. It is anticipated that from this comparison a correlation will begin to emerge between chemical structure, water interaction, and dynamic structure. Ultimately, based on work of this kind, it may be possible to understand the dynamics at carbohydrate linkages in terms of predicted microscopic interactions with water, and uncover the factors, which may have led to the evolution of oligosaccharide sequences.

## 2. Results and discussion

### 2.1. Rationale

Simulations were performed on oligosaccharide sequences that are found in glycoproteins, glycolipids, and proteoglycans (see Fig. 1 and the Experimental for details). These sequences contain both linear and branched chains, α and β linkages, and the sugars: mannose, glucose, galactose, and fucose. Some of the simulations have previously been compared against experimental data,[13–15] and their overall molecular conformations reported previously. Although it is theorized that dynamics of intramolecular hydrogen-bonds and water in the first solvation shell are important determiners of molecular conformation, no detailed analysis of hydrogen bonds and water structure has been performed on these oligosaccharides. Where strong water interactions are present, deviations may occur between predictions made in the presence of explicit water and those made on the basis of mean-field descriptions of water. In this case the TIP3P model for water was used, which has no explicit lone-pairs (as found in TIP5P, for exam-

ple) or polarizability.[19] The TIP3P water model is therefore one of the most basic, consisting of three point charges with an intrinsic bulk-water dipole moment. It is well-known that it exhibits less structuring than other models, and thus may underestimate hydrogen-bond strength and directionality.[20] However, since carbohydrate force-fields suitable for performing relatively long molecular dynamics simulations of oligosaccharides have not typically taken into account lone-pairs or polarizability, the TIP3P model, while not ideal, is currently the most suitable level of approximation.

A methodological step forward presented here is to compare these interactions in a variety of chemically distinct oligosaccharides. Using techniques that we have developed previously[21] (described in the Experimental) intramolecular hydrogen-bonds, single and dimer water-bridges across the linkages were extracted from each simulation; an aqueous simulation of glucose simulation concluded that water correlation only extends significantly for two shells.[11] In this current analysis, a hydrogen-bond was recorded if it was present for more than 2% of the simulation, while a water-bridge was considered if it was present for more than 10% of the time. Where an interaction was likely to be an important determiner of conformation, the equilibrium between hydrogen-bonded and water-bridged states was investigated.

### 2.2. α-Linked mannose

The core regions of glycans that are constituents of glycoproteins are often elaborated with α-linked mannose residues.[22] The first set of simulations were performed on model oligosaccharides containing mannose residues joined by α-(1→2), α-(1→3), and α-(1→6) linkages. Due to their importance in oligosaccharide structures,[2] for example, in N-linked glycans, these linkages will be discussed in detail. The first simulation to be analyzed was the pentasaccharide: Manα(1→3)Manα(1→3)Man α(1→3)Manα(1→2)Manα. Results from this simulation have been compared against experimental residual dipolar couplings and relaxation measurements,[15] and the basic parameters used to perform the simulations are shown in the Experimental. For the present purposes, initial analysis will be restricted to the fragment Manα(1→3)Manα(1→2)Manα, since it contains examples of both the important α-(1→2) and α-(1→3) linkages. The linkages will also be treated in isolation for simplicity, but the validity of this approach will be questioned by investigating longer range interactions. Figure 2 shows the chemical structure of this fragment, and interactions encountered frequently involving water molecules.

Analysis of the pentasaccharide simulation suggested that when the mannose α-(1→2) linkage is in its principal minima the direction of the sugar chain is changed

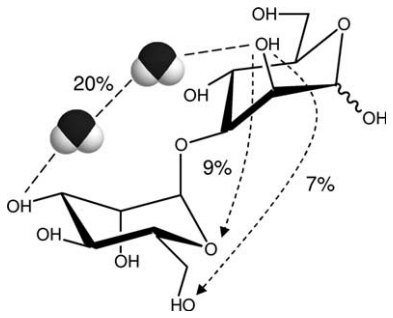


**Figure 2.** Hydrogen-bonds (shown by broken arrows, with percentage occupancy) and water-bridges predicted to exist at a Manα(1→3) Man linkage.

by almost 90°. This is because both bonds in the linkage are axial to the sugar ring planes, and leaves little possibility for direct interaction between adjacent mannose sugars residues. Therefore, no strong intramolecular hydrogen-bonds or water-bridges were observed across this linkage, indicating that there is little steric restriction to librations of the α-(1→2) linkage within its major minima, but as a consequence of the geometry, large rotations of the $\psi$ angle to 180° (see the Experimental for definitions) are energetically unfavorable. Within the global minimum there are two closely separated local minima,[15] at $(\phi,\psi) = (-50°, -20°)$ and $(-40°, 50°)$. The lack of direct interactions across this linkage explains why the α-(1→2) linkage can move rapidly between these two sub-minima, as reported previously,[15] and the simulation trajectory follows the in vacuo energy surface closely in water. Analysis of water structure, however, shows that the α-(1→2) linked mannose residue can interact with its next-nearest neighbor through hydrogen-bonds and single water-bridges, which happens to be an α-(1→3) linked mannose in this case. It is apparent that due to the directional change introduced by the α-(1→2) linkage, interactions are more likely possible beyond the nearest neighbor than with the adjacent neighbor. Analysis of these simulations suggested that interactions are mediated via the OH-3 hydroxyl of the α-(1→2) linked mannose to O-6 of the next-nearest neighbor, where both a hydrogen-bond (4% of the total simulation time) and a water-bridge (18%) are possible. Also, the reducing terminus, OH-1, is far from the linkage region, and thus the local water interactions at the linkage would not be expected to change significantly if the α-(1→2) linkage were to occur within the middle of an oligosaccharide, rather than at the reducing end.

In contrast, the relative orientation induced by the α-(1→3) linkage permits interactions between adjacent sugar residues. This is geometrically more favorable because the α-(1→3) linkage puts the two sugars in closer relative contact than the α-(1→2) linkage. It also permits the α-(1→3) linkage to flip into an alternative

conformation at $\psi = 180°$, which has been shown to be relatively unstable in simulations.[15] In what follows, the sugar closest to the nonreducing end will be identified by superscript ($i$), and then ($i + 1$), etc. for sugars that are successively toward the reducing end of the oligosaccharide. The predicted intramolecular hydrogen-bonds were from OH-2$^{(i)}$ to O-5$^{(i+1)}$ with a frequency of 9%, and to O-6$^{(i+1)}$ with a frequency of 7%; Table 1 details the frequency of all persistent interactions observed at this α-(1→3) linkage, and the plot in Figure 3 shows the relative orientation OH-2 and O-5 over the whole simulation. Within Figure 3 (top) three areas can be identified: the direct hydrogen-bond, a water-bridge, and water structure that corresponds to no effective interaction between the groups. Comparing conformational plots of the α-(1→2) and α-(1→3) linkages (Fig. 3 (middle and bottom)) shows that the conformational region at $(\phi, \psi) = (-40°, 50°)$, present at the α-(1→2) linkage, is shifted and weaker at the α-(1→3). The new region corresponds to the interaction between OH-2 and O-5, and is not present on the in vacuo adiabatic surface;[15] similar changes to the explored conformational space due to the effects of molecular water have been predicted for dixylose.[23] As we discussed previously, the equilibrium between hydrogen-bonds and water-bridges at carbohydrate linkages is, at present, not intuitive. It was proposed that this is because the favored configurations are not solely due to the molecular potential energy, but are also consistent with maximum rotamer and water degrees of freedom (configurational entropy).[12] The minima at $\psi = 50°$ is therefore less populated than in the α-(1→2) case because the OH-2 to O-5 hydrogen-bond is strained, and water-bridges, for some reason, are not stable at this position. Thus the equilibrium is between groups that are either hydrogen-bonded or decoupled (i.e., bridged by three or more water molecules)—the latter being favored in this case. The instability of water-bridges is not immediately apparent, but may be due to clusters of (nonpolar) CH groups that are located nearby. As a consequence, the sub-minima at ($\phi$, $\psi$) = (−50°, −20°) is predicted to be more highly populated than at the α-(1→2) linkage, making the α-(1→3) linkage less dynamic locally. No strong single water-bridges were predicted at this linkage, but the distance between groups is suited to dimer water-bridges (Fig. 2). Table 1 shows that interactions can occur between several hydroxyls via two water molecules. These interactions, however, have many permutations and have little effect on the dynamic conformation at the linkage. In

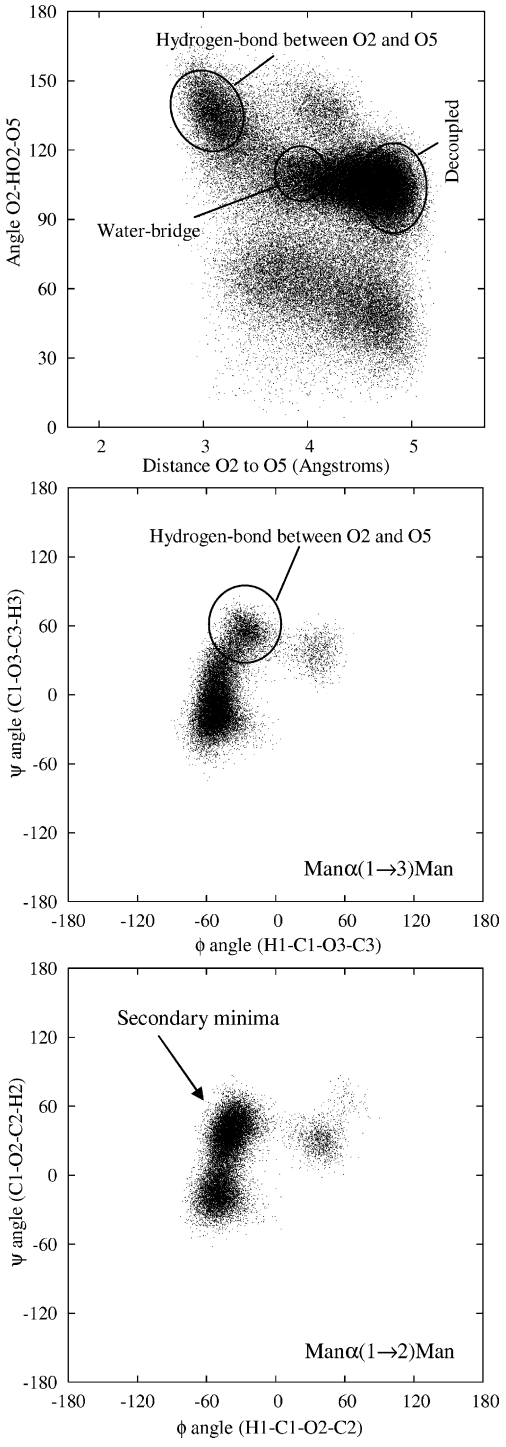


**Figure 3.** Top. Relative orientation of the OH2 and O5 moieties across the Manα(1→3)Man linkage. Middle. Predicted exploration of the Manα(1→3)Man linkage in water. Bottom. Predicted exploration of the Manα(1→2)Man linkage in water.

**Table 1.** Percentage occupancy of hydrogen-bonds and water-bridges at a Manα(1→3)Man linkage

| Sugar ($i$) | Sugar ($i + 1$) | Hydrogen-bond (%) | Water-bridge (%) | Dimer water-bridge (%) |
|---|---|---|---|---|
| O-2 | O-5 | 9 | 1 | 0 |
| O-2 | O-6 | 7 | 4 | 5 |
| O-2 | O-4 | 0 | 2 | 20 |
| O-4 | O-2 | 0 | 0 | 11 |

Sugars $i$, $i + 1$ are successively toward the reducing end of the oligosaccharide.

common with the α-(1→2) linkage interactions are possible between next-nearest neighbors, and was investigated by considering another fragment from the full pentasaccharide, namely the trisaccharide Manα(1-3)Manα(1→3)Manα. The most probable water interactions were between OH-$2^{(i)}$ and OH-$4^{(i)}$ to O-$6^{(i+2)}$ with frequencies of 11 and 16%, respectively. Therefore, α-(1→3) linked mannose residues are likely to make interactions between both nearest and next-nearest neighbors, and potentially longer range interactions in branched structures.

The branch points that form the antennae of oligomannose structures often involve α-(1→6) linkages, and they are therefore of fundamental importance to understanding N-linked glycans. A previous simulation of the branched trisaccharide Manα(1→3)[Manα(1→6)]Manα was used to investigate water interactions at the α-(1→6) linkage. Analysis suggested that no significant interaction occurred between the mannose residues in the two branches, which may not be the case in larger oligosaccharides.[24] Therefore, the α-(1→6) linkage was considered in isolation (Fig. 4). Previous studies using residual dipolar couplings had indicated that both the *gg* and the *gt* conformation are possible at the α-(1→6) linkage with almost equal populations.[14] In a 50 ns simulation examples of both the *gg* and *gt* conformations were found, and were stable for sufficient periods of time to allow their individual analysis. Rotation around this linkage causes large changes in overall conformation, and each conformer is predicted to possess a distinct water structure. In the *gg* conformation no intramolecular hydrogen-bonds were observed. However, a water bridge was observed with a frequently

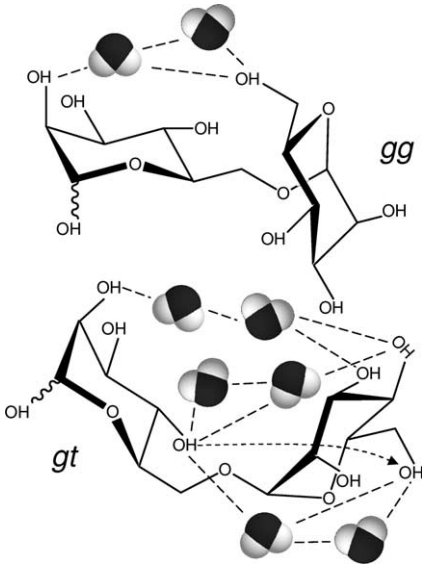


**Figure 4.** Hydrogen-bond (shown by a broken arrow) and water-bridges predicted to exist at a Manα(1→6)Man linkage in two different predicted conformations, the *gg* (top) and *gt* (bottom).

of 12% between the O-$2^{(i+1)}$ and O-$6^{(i)}$ moiety (see Fig. 4); in this case ($i$ + 1) represents the terminal α-(1→6) linked mannose. Even more frequently (20%) a dimer water-bridge was observed between these groups, indicating that they are, on average, relatively distant from one another. Therefore, it is anticipated that predictions of the conformational space explored made in vacuo will be similar to those made with water present, for the α-(1→6) linkage in the *gg* conformation. In the *gt* conformation a weak direct hydrogen-bond was found between O-$4^{(i+1)}$ and O-$6^{(i)}$ for 2% of the total time. The hydrogen-bond could be bridged by both single (18% of the time) and pairs of water molecules (28% of the time). Another water-bridge was predicted between O-$4^{(i+1)}$ and O-$4^{(i)}$ with frequencies of 13 and 28% for single and dimer water-bridges, respectively. Longer range interactions that could maintain only dimer water-bridges were also found from O-$2^{(i+1)}$ to O-$3^{(i)}$ (17% of the time) and to O-$4^{(i)}$ (13% of the time). Therefore, it is the *gt* conformation that possesses the largest number of intramolecular hydrogen-bonds and ordered water molecules, and is more dependent on the effects of molecular water than the *gg* conformer.

Oligomannose structures with α-(1→2) and α-(1→3) linkages are key components of N-linked glycans. Previous simulations of the biosynthetic precursor of mature N-linked glycans,[25] $Man_9GlcNAc_2$, combined with NMR data suggested that the conformation of the α-(1→2) linkages were inconsistent with a single conformation.[26,27] Similar results were obtained for α-(1→3) linked mannose sugars.[14,28] However, based on simulations and NMR analysis of a penta-antennary glycan it was concluded that linkages in the core of the oligosaccharide had a limited overall torsional oscillation, with the α-(1→6) linkage being a notable exception.[29] In that study, and one of a related bi-antennary glycan, the linkages were predicted to be in their global minima but had a further restriction as a direct result of steric restriction due to the other substituents.[30] Therefore, simulations show that interactions can occur between noncontiguous residues in regions of α-linked mannose residues, and that deriving oligomannose conformations based on the conformational preferences of the constituent disaccharide fragments will not always yield correct results.[31] Based on the simulation data presented here an attempt can be made to rationalize these results. Firstly, due to the prevalence of long-range water interactions, the α-(1→2) linkage is predicted to rapidly explore large regions of its conformational space, but only within its primary minima. Secondly, the α-(1→3) linkage is predicted to have a more restricted exploration of its major minima, due to water structuring around a single hydrogen-bond, but has the possibility to explore a secondary minima,[15] which was not investigated here. Thirdly, the α-(1→6) linkage was predicted to be highly solvated with many weak water-bridges and hence should explore

its conformational space rapidly, and in a similar fashion to that expected on the basis of in vacuo calculations. Finally, these simulations suggest that α-linked mannose residues have a high propensity to interact with noncontiguous residues, and particularly when α-(1→2) and α-(1→6) linkages are present.

### 2.3. α-Linked glucose

The oligosaccharide transferred en-bloc to recipient asparagines in nascent glycoproteins within the endoplasmic reticulum is $Glc_3Man_9GlcNAc_2$. The terminal glucosyl residues are subsequently trimmed and provide important recognitions motifs for membrane bound proteins such as the molecular chaperone calnexin.[25] A simulation of Glcα(1→2)Glcα(1→3)Glcα(1→3)Manα was performed to investigate water interactions in these glucose oligosaccharides, and in this case the results have not been published previously. Figure 5 shows the α-(1→3) linkage between Man and Glc. Here the epimerization state of the sugars is different to the α-(1→3) linkage studied above and this is reflected in the predicted hydrogen-bonding interactions. In common with the Manα(1→3)Man linkage the hydrogen-bond from OH-$2^{(i+1)}$ to O-$5^{(i)}$ is a geometric possibility, and is observed with a low frequency of 4%. The orientation of this hydrogen-bond over the whole simulation is shown in Figure 6. Comparison with Figure 3 shows that similar water dynamics exist around this hydrogen-bond, and it is most commonly in an orientation where no hydrogen-bond or water-bridge exists; thus the two groups are largely decoupled. On the other side of the linkage a hydrogen-bond, between OH-$4^{(i+1)}$ and O-$2^{(i)}$, is orientationally possible. However, it is predicted to have a low probability (5%), and inspection of Figure 6 shows that it favors the singly water bridged orientation (for 33% of the time), similar to that seen in xylan,[12] and also dimer water-bridges (for 21% of the time). Although this is one of the most stable single water-bridges yet observed in simulations, exchange can still occur relatively freely. Figure 7 shows a graph of water molecules that bridge the linkage over a

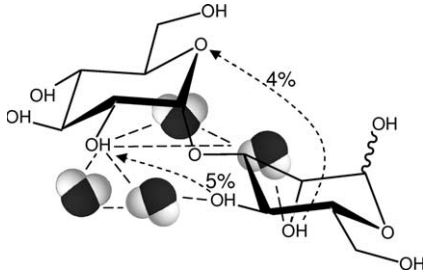


**Figure 5.** Hydrogen-bonds (shown by broken arrows, with percentage occupancy) and water-bridges predicted to exits at a Glcα(1→3)Man linkage.

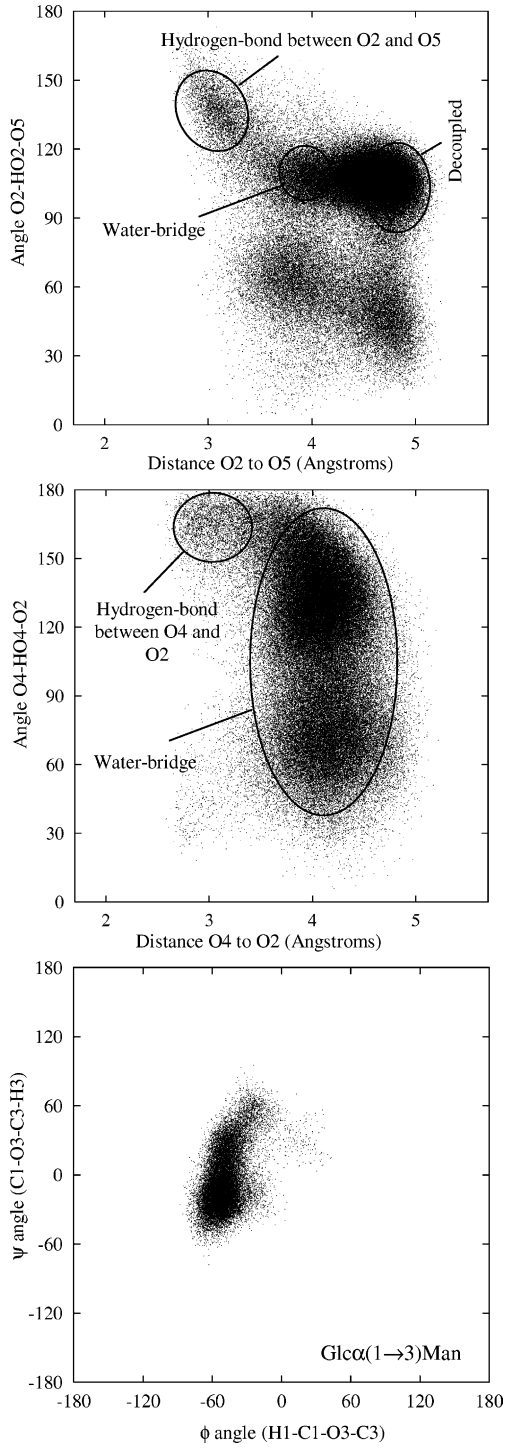


**Figure 6.** Top. Relative orientation of the OH2(Man) and O5(Glc) moieties across a Glcα(1→3)Man linkage. Middle. Relative orientation of the OH4(Man) and O2(Glc) moieties across a Glcα(1→3)Man linkage. Bottom. Predicted exploration of the Glcα(1→3)Man linkage in water.

0.5 ns period; no water molecule is in residence for more than 0.1 ns. It is proposed that this water-bridged situation is consistent with both the conformationally accessible space at the α-(1→3) linkage and the most likely

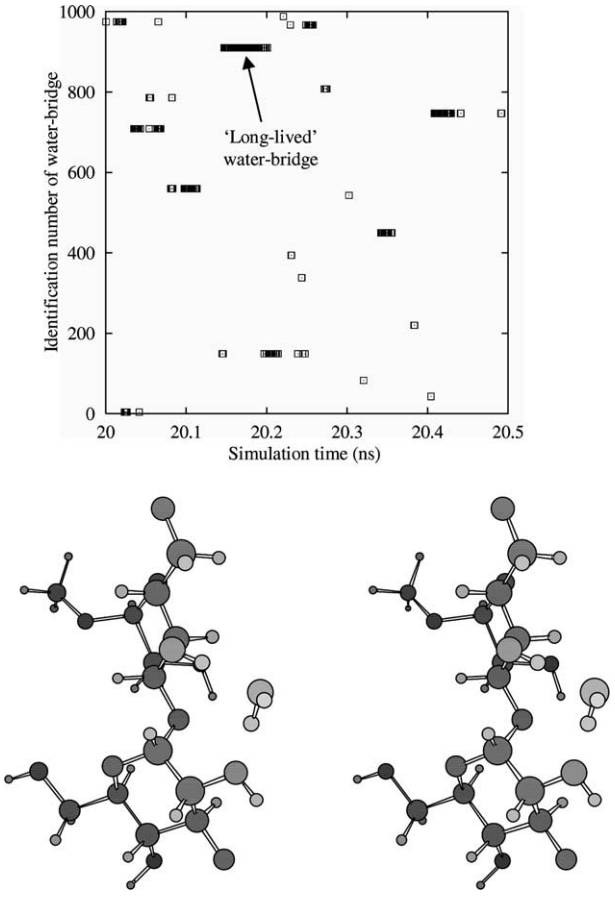


**Figure 7.** Top. Residence times of particular water molecules between O4(Man) and O2(Glc) at the Glcα(1→3)Man linkage, over a 0.5 ns section of a simulation in aqueous solution. Bottom. Stereo image showing a typical water bridging the Glcα(1→3)Man linkage.

conformation at the OH-2 to O-5 hydrogen-bond, which has less flexibility because it cannot form single or dimer water-bridges. The occupancy of hydrogen-bonds and water-bridges at this linkage are presented in Table 2, and Figure 7 shows a stereo representation of the water-bridge between OH-4 and O-2. Water-bridges were also found between O-2$^{(i+1)}$ and O-2$^{(i)}$ with a frequency of 24%, and dimer water bridges with frequency 18%. Also water-bridges are observed between O-3$^{(i+1)}$ and O-2$^{(i)}$ with frequency 20%, but in this case dimer water-bridges have a low probability, 3%. Therefore, the conformational exploration of this linkage is similar to the fully mannose case—compare Figures 3 and 6.

**Table 2.** Percentage occupancy of hydrogen-bonds and water-bridges at a Glcα(1→3)Man linkage

| Sugar ($i$) | Sugar ($i+1$) | Hydrogen-bond (%) | Water-bridge (%) | Dimer water-bridge (%) |
|---|---|---|---|---|
| O-2 | O-5 | 4 | 0 | 0 |
| O-4 | O-2 | 5 | 33 | 21 |
| O-2 | O-2 | 0 | 24 | 18 |

Sugars $i$, $i+1$ are successively toward the reducing end of the oligosaccharide.

In the triglucosyl cap structure examples are found of both α-(1→2) and α-(1→3) linked glucose. As can be seen in Figure 8 formation of this structure, and epimerization of the O-2 groups from mannose to glucose, has a dramatic effect on the exploration of the individual

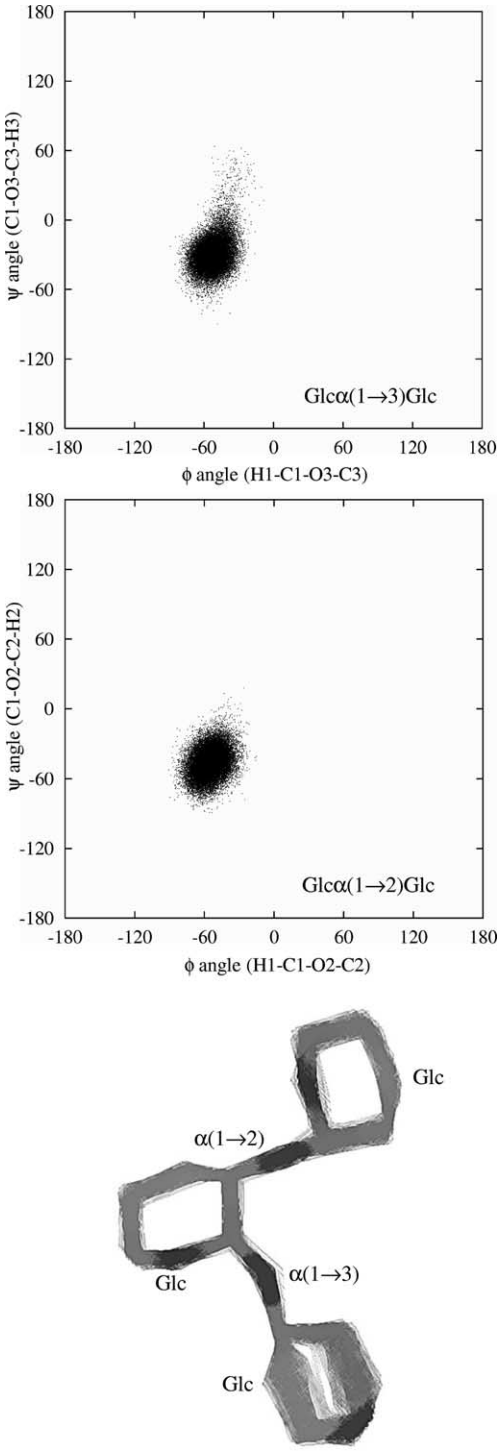


**Figure 8.** Top and middle. Predicted exploration of the Glcα(1→3)Glc and Glcα(1→2)Glc linkage within an oligosaccharide containing the triglucosyl motif Glcα(1→3)Glcα(1→2)Glc. Bottom. Overlay of a 50 ns simulation of Glcα(1→3)Glcα(1→2)Glc in aqueous solution.

linkages. In this case the sub-minima at $(\phi,\psi) = (-40°, 50°)$ is virtually excluded (Fig. 8). Interestingly, analysis of hydrogen-bonds shows that they are rarely predicted between neighboring residues. Also, water bridges are infrequently observed between neighboring sugars residues, the interaction between O-3$^{(i+1)}$ and O-2$^{(i)}$ across the α-(1→3) linkage being a minor exception, with a frequency of 11%. Dimer water-bridges are more probable, due to the relatively large distance between donors and acceptors. Across the α-(1→2) linkage O-2$^{(i+1)}$ can interact with O-2$^{(i)}$, frequency 18%, and O-4$^{(i)}$, frequency 22%, whilst across the α-(1→3) linkage O-4$^{(i)}$ to O-2$^{(i+1)}$ occurs with a frequency of 26%.

The result of these interactions is a relatively tight structure, and further investigation reveals that the two next-nearest neighbors in the trisaccharide almost stack together to exclude water. Therefore, in this case it is not possible to treat the two linkages in isolation, because interactions between next-nearest neighbors are prevalent. In particular, hydrogen-bond interactions are consistent with the tight conformation adopted, namely: OH-4$^{(i+2)}$ to O-2$^{(i)}$ (frequency 10%), and OH-2$^{(i)}$ to O-4$^{(i+2)}$ (frequency 3%); see Figure 8 (bottom) for a dynamic overlay of the trisaccharide. It should be noted that for these interaction to occur, O-2 has to have an equatorial configuration—so they would not occur in a mannose trisaccharide with the same sequence of linkages. Water-bridges (single and dimer) were also found to connect O-2$^{(i)}$ to the next-nearest sugar residue through O-2$^{(i+2)}$, O-3$^{(i+2)}$, O-4$^{(i+2)}$, and O-6$^{(i+2)}$. Based on this analysis it is clear that O-2 on the terminal glucosyl sugar residue has a pivotal role in determining the water structure and conformation of the triglucosyl cap.

Previous NMR experiments observed only one NOE at each glycosidic linkage of the triglucosyl cap,[32] compared to three or four typically across mannose linkages. The absence of NOEs was interpreted as a single rigid conformation at each of the linkages, and is consistent with the molecular dynamics simulation analyzed here (Fig. 8), which indicates a crucial role for the O-2$^{(i)}$ to O-4$^{(i+2)}$ hydrogen-bond. Also, the rigidity of these residues is probably essential for their biological function, as there would be a minimal entropic penalty for formation of the ordered protein bound state. A similar rigidity was found in simulations of fucosylated epitopes,[13] which are also involved in binding to proteins. In both of these cases stacking of the sugar rings, resulting in exclusion of water, may be involved in driving the structure toward an ordered conformation.

### 2.4. α-Linked fucose

Fucose sugars, distinct in being the L-enantiomers, are often found as part of oligosaccharide sequences and are essential components of the Lewis blood group epitopes.[33] Their biological importance has led to many previous studies of conformation using molecular dynamics simulations, but without explicit solvent.[34–38] Human milk is unique in containing large amounts of these fucosylated complex oligosaccharides, which act as protection for nursing infants against pathogens.[39] Structurally they consist of lactose elaborated with termini similar to those present on glycoconjugates.[40] Simulations were performed on the lactose-containing trisaccharide Fucα(1→2)Galβ(1→4)Glc, which has been subjected to experimental testing using residual dipolar couplings and relaxation.[13] Analysis of the simulation revealed that no hydrogen bonds, and only weak water-bridges, could be formed between the first and last sugar residues. In the three-dimensional structure the sugars are in close proximity, and form a pocket, that is, essentially excluded from water. This region is demarcated by the H-1/H-3/H-5 face of the Glc together with the H-5 and methyl of the Fuc sugar, all nominally non-polar groups. Analysis of the β-(1→4) linkage reveals that an extremely strong hydrogen-bond is predicted to bridge it, namely OH-3(Glc) to O-5(Gal), with a frequency of 58%. Here single and dimer water-bridges had a persistence of 19 and 4%, respectively. This is a much larger hydrogen-bond frequency than was observed across α linkages, where the value is predicted to be less than about 10%. The α-(1→2) Fuc linkage is a case in point, where a hydrogen-bond is predicted between OH-3(Gal) to O-2(Fuc) with a frequency of 10%, and OH-2(Fuc) to O-3(Gal) with a frequency of 5%; compared to other α linkages studied the interaction is actually relatively strong. Table 3 details the frequency of hydrogen-bonds and water-bridges at this linkage. The O-2 moiety is also involved in single and dimer water-bridges to O-3(Gal) with frequencies of 13 and 15%, respectively, and are similar in occupancy to the intramolecular hydrogen-bond; a methyl group on the fucose residue ensures that water interactions are restricted to the O-2 side of the linkage. These interactions, together with the potential at the glycosidic linkages, result in an α-(1→2) linkage that is confined to a single region of conformational space, as proposed previously.[41,42] Figure 9 displays a plot of the geometry at the hydrogen-bond between OH-2 and O-3, showing the equilibrium between directly hydrogen-bonded and water-bridged states, and a comparison with the hydrogen-bond be-

**Table 3.** Percentage occupancy of hydrogen-bonds and water-bridges across a Fucα(1→2)Gal linkage

| Sugar 1 | Sugar 2 | Hydrogen-bond (%) | Water-bridge (%) | Dimer water-bridge (%) |
|---|---|---|---|---|
| O-2(Fuc) | O-3(Gal) | 15 | 13 | 15 |
| O-3(Glc) | O-5(Gal) | 58 | 19 | 4 |

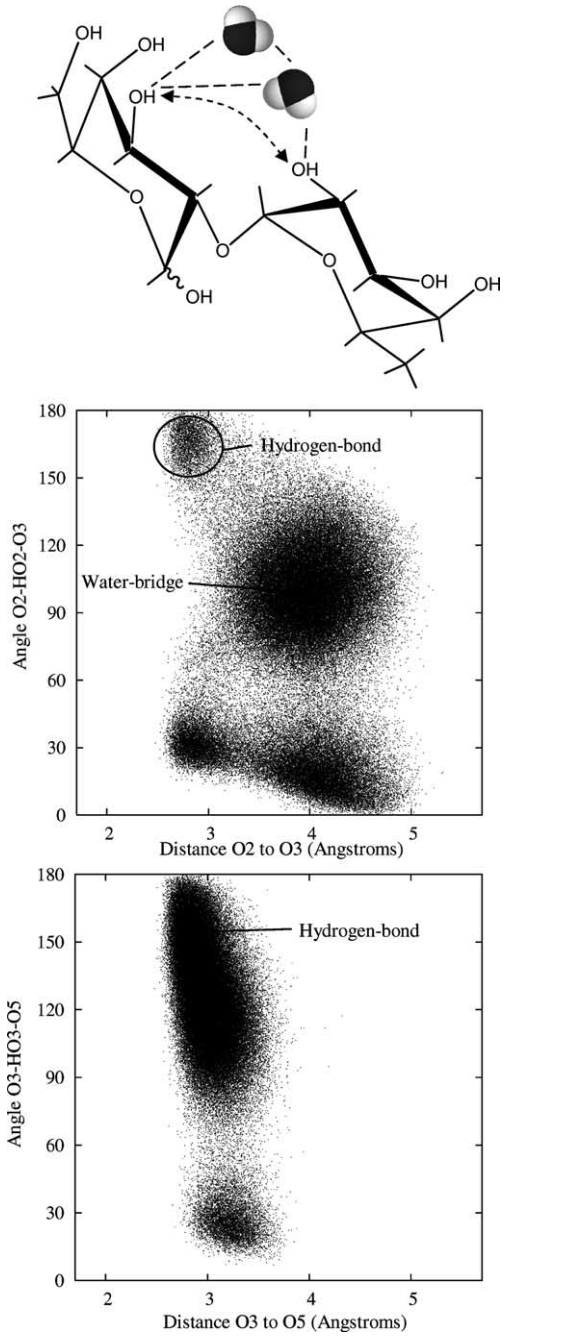


**Figure 9.** Top. Hydrogen-bonds and water-bridges predicted to exist at a Fucα(1→2)Gal linkage. Middle. Relative orientation of the OH2(Fuc) and O3(Gal) moieties across a Fucα(1→2)Gal linkage. Bottom. Relative orientation of the OH3(Glc) and O5(Gal) moieties across a Galβ(1→4)Glc linkage.

tween OH-3 and O-5 across the β-(1→4) linkage. Figure 10 shows a stereo image of the fucose trisaccharide with a hydrogen-bond at the β-(1→4) linkage and a water-bridge at the α-(1→2). From this it is clear that the dynamics of water around the β-(1→4) linkage is significantly different to that around the fucose α-(1→2) linkage. The former favoring a direct hydrogen-bond while the latter prefers a water-bridge. It is proposed that these differences are determined by the geometry (and potential energy) associated with the linkage and water interactions that maximize total rotational degrees of freedom.

### 2.5. Glycosaminoglycans

Oligosaccharides that are components of glycoproteins, and are thought to have predominantly recognition roles, often contain many α linkages (to 2-, 3-, and 6-position). However, the glycosaminoglycans hyaluronan and chondroitin, considered to be primarily structural molecules, are made up exclusively from β linkages (to 3- and 4-position).[43,44] Both glycosaminoglycan molecules are ubiquitous components of the mammalian extracellular matrix; hyaluronan is normally found free and chondroitin (sulfate) is attached to protein as a component of proteoglycan molecules. It has been alluded to already that β linkages are predicted to have strong intramolecular hydrogen-bonds between the neighboring sugar residues, whereas α linkages prefer water-bridges. To investigate whether there could be a correlation between β linkages and three-dimensional structure, simulations were performed on the glycosaminoglycans hyaluronan and chondroitin. In order to compensate for the intrinsic charge of these molecules, charge balancing sodium ions were added to each simulation. Chemically the glycosaminoglycans are repeats of a disaccharide consisting of an *N*-acetylated and a uronic acid sugar residue, and thus the interactions at the linkages are repeated throughout the structure. In the case of hyaluronan, a simulation was performed on the tetrasaccharide GlcAβ(1→3)GlcNAcβ(1→4)GlcAβ(1→3)-GlcNAcβ; the dynamic conformation of similar oligosaccharides, and testing against experimental data, have been reported previously.[17,18] Analysis of the current simulation revealed that at the β-(1→3) linkages there are hydrogen-bonding interactions from GlcNAc OH-4 to GlcA O-5 (frequency 40%), and from GlcA OH-2 to GlcNAc O-7 (frequency 28%). Similarly, at the β-(1→4) linkage the prominent hydrogen-bonding interactions are GlcNAc HN to GlcA O-6 (frequency 22%), and GlcA OH-3 to GlcNAc O-5 (frequency 49%); Table 4 details these results. The strongest interactions at both linkages are from a hydroxyl to an adjacent ring oxygen, as observed in the lactose disaccharide, and in other polysaccharides,[12] where a reductionist explanation based on water molecules was proposed. Clearly, these are much stronger interactions that those typically found at α linkages, and again are suggestive of vastly different water dynamics at the two types of linkages. Figure 11 shows the chemical structure of the hyaluronan oligosaccharide, and the most likely water and hydrogen-bond interactions. Two interactions involving water-bridges were found at the β-(1→3) linkage: between GlcNAc O-7 and GlcA

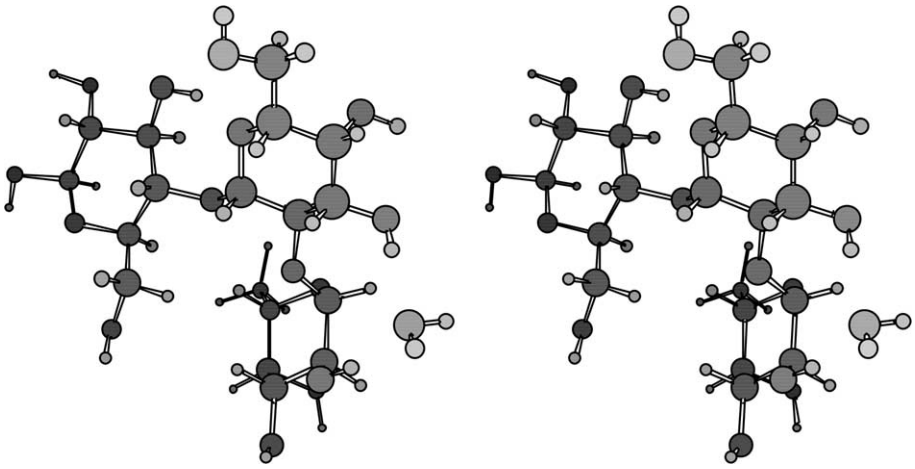

**Figure 10.** Stereo image of the trisaccharide Fucα(1→2)Galβ(1→4)Glc, showing a water molecule bridging α-(1→2) linkage and the direct hydrogen-bond bridging the β-(1→4) linkage.

**Table 4.** Percentage occupancy of hydrogen-bonds and water-bridges across the GlcAβ(1→3)GlcNAc and GlcNAcβ(1→4)GlcA linkages in hyaluronan

| Sugar 1 | Sugar 2 | Hydrogen-bond (%) | Water bridge (%) | Dimer water-bridge (%) |
|---|---|---|---|---|
| O-2(GlcA) | O-7(GlcNAc) | 28 | 24 | 23 |
| O-4(GlcNAc) | O-6(GlcA) | 0 | 19 | 74 |
| O-4(GlcNAc) | O-5(GlcA) | 35 | 8 | 4 |
| N(GlcNAc) | O-6(GlcA) | 23 | 58 | 49 |
| O-3(GlcA) | O-5(GlcNAc) | 49 | 14 | 4 |

O-2 (single 24%, dimer 23%), and from GlcNAc O-4 to GlcA O-6 (single 19%, dimer 74%). It is noted that the latter interaction has an extremely high residence of dimer water-bridges at 74%, being present virtually all of the time. At the β-(1→4) linkage strong water-bridges were predicted between GlcNAc N and GlcA O-6 (single 58%, dimer 49%), and GlcA O-3 to GlcNAc O-5 (single 14%, dimer 4%). Therefore, both hydrogen-bonds and water-bridges are more frequent at the β-(1→4) linkages. A water-bridge has previously been proposed to exist between the amide and carboxyl on the basis of NMR and molecular modeling,[45] and a typical frame extracted from the simulation where this is the case is shown in the stereo image of Figure 11.

In chondroitin the GlcNAc residues are epimerized to GalNAc, and the structure is also often sulfated, but this will not be considered here. Epimerization is predicted to affect the hydrogen-bonding patterns and water structure at the β-(1→3) linkage, which may be key to understanding why hyaluronan and chondroitin have a similar backbone chemistry, but very different biology. In chondroitin hydrogen-bonds were predicted at the β-(1→3) linkage. However, they changed their frequency of observation, compared to hyaluronan. The GalNAc OH-4 to GlcA O-5 hydrogen-bond had a frequency of 9%, down from 40% in hyaluronan. Conversely, the GlcA OH-2 to GalNAc O-7 hydrogen-bond, with a frequency of 43%, is less probable in hyaluronan, where it was found only 24% of the time; compare Tables 4 and 5. Figure 11 shows the chemical structure of the chondroitin tetrasaccharide and the likely hydrogen-bonds and water interactions. It can be seen that strong water-bridges were observed at the β-(1→3) linkage, for example, from GalNAc O-7 to GlcA O-2, and GalNAc O-4 to GlcA O-2. In general the β-(1→4) linkage was found to have similar hydrogen-bonding dynamics in both hyaluronan and chondroitin. For example, the hydrogen-bond from GlcA OH-3 to GalNAc O-5 had a frequency of 48% in chondroitin as compared to 49% in hyaluronan, and water interactions across the β-(1→4) were similar to those in hyaluronan, in agreement with the linkage exploration being the same in the two cases. However, at the β-(1→3) linkage water-bridges between O-4(GalNAc) and O-6(GlcA) had a reduced intensity, with single and dimer water bridges having frequencies of 1 and 13%, respectively. Therefore, the GalNAc OH-4 and GlcA O-5 become decoupled from one another, and the β-(1→3) linkage is dominated by the interaction between GlcA O-2 and GalNAc O-7, whereas in hyaluronan it also accommodates the GalNAc OH-4 and GlcA O-5 hydrogen-bond, and this results in a conformational shift at the linkage, as was observed in previous studies.[16] Figure 12 shows the orientation of the O-4 hydrogen-bond and also the effect on the conformation of the β-(1→3) interactions. Therefore, epimerization of the OH-4 moiety changes the water dynamics at the β-(1→3), resulting in a breaking of the OH-4 to O-5 hydrogen-bond, and a strengthening of the hydrogen-bond on the other side of the linkage. This produces a shift in conformation, but not a large change in the amount of conformational exploration at the linkage, and suggests that the strong hydrogen-bonds between hydroxyl and ring oxygen often

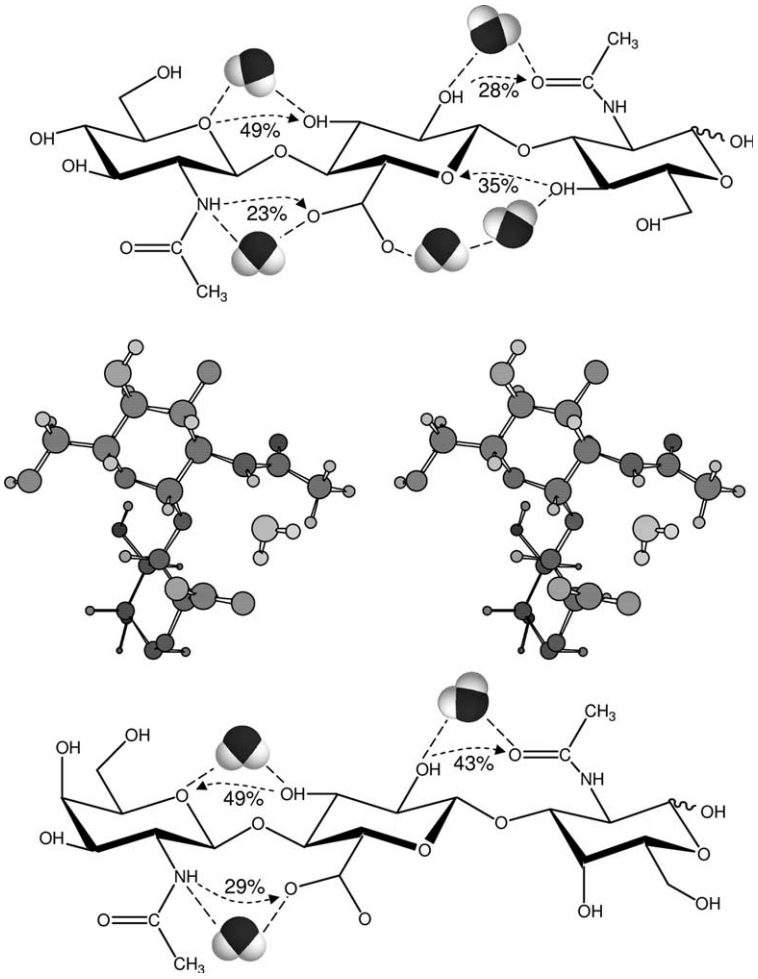


**Figure 11.** Top. Hydrogen-bonds and water-bridges predicted to exist in the hyaluronan tetrasaccharide: GlcAβ(1→3)GlcNAcβ(1→4)GlcAβ(1→3)GlcNAc. Middle. Stereo image of a water molecule bridging amide and carboxyl at the β-(1→4) linkage of the hyaluronan molecule. Bottom. Hydrogen-bonds and water-bridges predicted to exist in the chondrotin tetrasaccharide: GlcAβ(1→3)GalNAcβ(1→4)GlcAβ(1→3)GalNAc.

**Table 5.** Percentage occupancy of hydrogen-bonds and water-bridges across the GlcAβ(1→3)GalNAc and GalNAcβ(1→4)GlcA linkages in chondroitin

| Sugar 1 | Sugar 2 | Hydrogen-bond (%) | Water bridge (%) | Dimer water-bridge (%) |
|---|---|---|---|---|
| O-2(GlcA) | O-7(GalNAc) | 43 | 22 | 19 |
| O-4(GalNAc) | O-6(GlcA) | 0 | 1 | 13 |
| O-4(GalNAc) | O-5(GlcA) | 9 | 3 | 4 |
| N(GalNAc) | O-6(GlcA) | 29 | 61 | 47 |
| O-3(GlcA) | O-5(GalNAc) | 49 | 25 | 7 |

found at β linkages are a feature of equatorial hydroxyls. The fact that OH-4 is no longer involved in intramolecular interactions is consistent with it being a target for sulfation in chondroitin sulfate.

## 2.6. Summary

The equilibrium between water excluded regions such as hydrogen-bonds and hydrophobic pockets, partially solvated water-bridges, and freely solvated groups has been studied here. An understanding of these water-dependent properties is key to determining the conformation and dynamics at glycosidic linkages, is central to the function of oligosaccharides and polysaccharides, and may help to explain why certain sequences of sugars have been selected during evolution at the expense of others.

When mannose is α-(1→2) linked there are virtually no interactions between contiguous residues via hydrogen-bonds or water-bridges, and hence the energy surface is explored rapidly within the primary minima, almost reproducing the in vacuo behavior. Interactions may, however, occur between nonadjacent sugar residues, even within linear chains. In contrast, when the mannose residues are linked by an α-(1→3) the linkage is more constrained because of specific water and hydrogen-bond interactions between adjacent sugars, not present at the α-(1→2) linkage and not predicted in vacuo. Also, there is additional possibility for large conformational changes to $\psi = 180°$, but these conformers are predicted be unstable.[15] Substitution of one of the

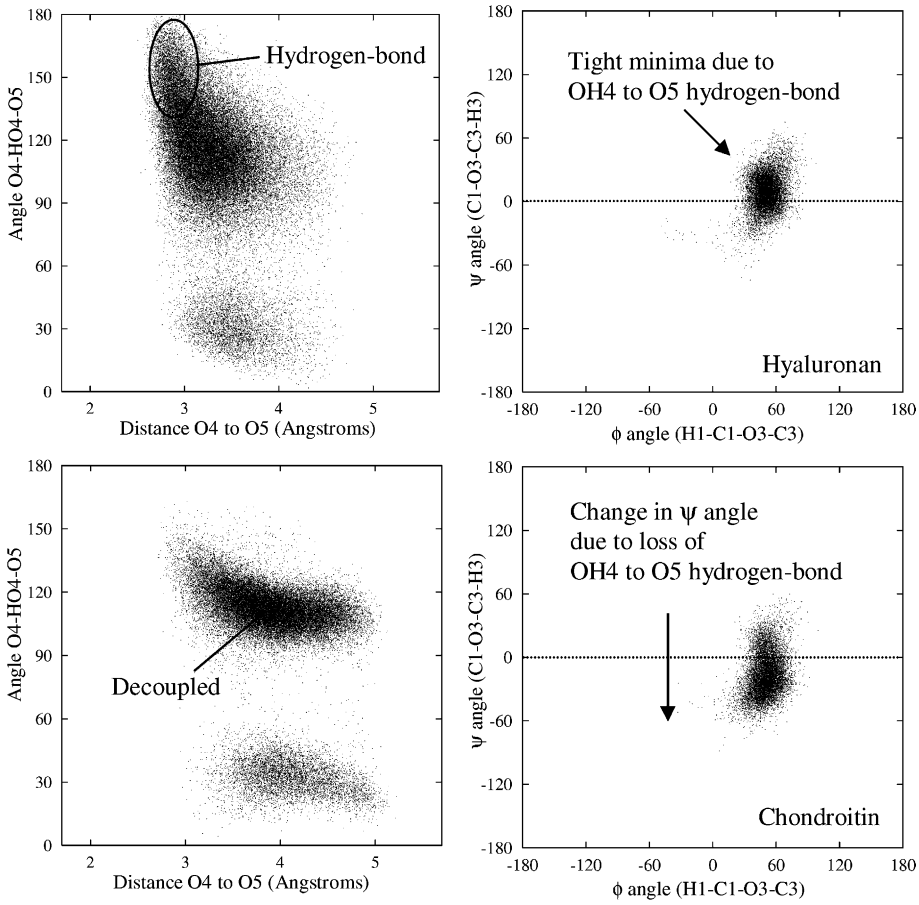


**Figure 12.** Top. Relative orientation of the OH4(GlcNAc) and O5(GlcA) moieties across the β-(1→3) linkage in hyaluronan, and the predicted exploration of this linkage. Bottom. Relative orientation of the OH4(GalNAc) and O5(GlcA) moieties across the β-(1→3) linkage in chondroitin, and the predicted exploration of this linkage.

mannose residues (toward the nonreducing end) for a glucose leaves this dynamic behavior unaltered, and sequences of sugars linked by α-(1→2) and α-(1→3) linkages are likely to interact with each other via noncontiguous residues. At mannose α-(1→6) linkages, few interactions were observed between adjacent sugars, indicating that the linkage exploration would be similar to that predicted in vacuo. However, more water interactions are predicted in the *gt* conformation, which is the least extended, and is also the most likely to interact with nonadjacent sugar residues in oligosaccharides.

In the triglucosyl cap, found in nascent glycoproteins, interactions occurred between nonadjacent sugar residues to exclude water and form a tight conformation. At the terminal glucose an important hydrogen-bonding and water structuring role was found for the equatorial O2. Similarly, in α-(1→2) linked fucose the O2 hydroxyl was predicted to be involved in hydrogen-bonds and water interactions to the oligosaccharide core residues. The opposite side of the α-(1→2) fucose linkage has a methyl moiety, and is predicted to form a hydrophobic pocket involving the nonpolar planar faces of nearby sugar residues.

The glycosaminoglycans hyaluronan and chondroitin are fully β linked, and form strong hydrogen-bonds across their linkages. These are OH3 to O5 and amide to carboxyl at β-(1→4) linkages, and OH2 to carbonyl at β-(1→3) linkages. However, hyaluronan was predicted to have an additional strong hydrogen-bond involving equatorial OH4, which is not present in chondroitin because the OH4 group is axial. This hydrogen-bond is not replaced by water-bridges, and results in conformational change at this linkage.

In conclusion, it was found that α linkages in oligosaccharides maintain weak hydrogen-bonds across their linkages, and possess many water bridges, with inherent conformational mobility. Due to their geometry they also have a tendency to interact with noncontiguous residues, and perhaps form compact secondary structure by packing and excluding water. Therefore, it may not be sufficient to model these linkages in isolation. On the other hand, β-linkages were found to have strong hydrogen-bonds across the linkages. Hydrogen-bonds involving equatorial hydroxyls and ring oxygens are persistent and have water structure around them that is dependent on nearby substituents. The resultant secondary

structures were found to be extended and explore relatively small regions of conformational space.

The observations made for the linkages investigated here appear well correlated with their biological functions. The α linkages from oligosaccharides were involved in many water interactions, resulting in dynamic mobility; taken together with their ability to form compact, branched structures this allows mannose containing oligosaccharides to partake in multivalent interactions with proteins. However, the β linkages considered here formed extended, and relatively rigid, structures suitable for structural molecules, and are only found at the attachment site of oligosaccharides to proteins (e.g., in N-linked glycans) where the oligosaccharide needs to clear the protein surface, and at their nonreducing termini. These results therefore begin to provide a relationship between chemical structure, water interactions and the function of specific sugars and linkages.

## 3. Experimental

### 3.1. Molecular dynamics simulations

Simulations were performed on the six oligosaccharides shown schematically in Figure 1. All simulations were performed with a force-field suitably modified for carbohydrates,[46] and using the molecular dynamics simulation software CHARMm.[47] In all cases the TIP3P model for water was used, which uses three point charges.[19] In simulations **1** through **4** water was modeled using periodic boundary conditions tessellated in the face-centered cubic arrangement with the relevant Wigner–Seitz cell unit (a rhombic dodecahedron). Nonbonded interactions were cut-off using the switching function between 0.8 and 1.2 nm, and the dielectric was maintained at the vacuum value ($\varepsilon_0$). Simulations were run in the NVT ensemble (since no change in volume is expected) using the leap-frog modification of the Verlet algorithm with a time-step of 2 fs, and a temperature of 298 K by weak coupling to a heat-bath (coupling constant 5 $ps^{-1}$). Prior to the production dynamics run 200 ps of equilibration was performed, by strong coupling to a heat bath. Nonbonded lists and images were updated frequently (every five steps) to maintain energy conservation. The size of the central unit cell and number of water molecules for each simulation was: (**1**) 3.9964 nm, 1500 waters, (**2** and **4**) 3.4912 nm, 1000 waters, (**3**) 4.50 nm, 2141 waters. In each case water molecules were discarded to make room for the solute and to maintain correct volume and pressure, as described previously.[20] For simulations **5** and **6** rhombic dodecahedral periodic boundary conditions were used, and the central unit cell had a size of 4.0 nm, which initially contained 1504 water molecules and two sodium ions (to achieve charge neutrality). To take account of the increased simulation complexities of introducing carboxylic acid moieties and sodium ions, the long range electrostatics were calculated using the particle mesh Ewald (PME) summation, and pressure (NPT ensemble), rather than volume (NVT ensemble) was kept constant; the incompressibility of water ensures that the two approaches produce comparable results. The simulations of **5** and **6** employed the leap-frog Verlet algorithm, with a time-step of 2 fs, and the pressure (1 atm) and temperature (298 K) were kept constant using the Nosé–Hoover algorithm with suitable masses. The PME parameters were $\kappa = 0.33$, an order of 6, and an fft size of 64 in each dimension. Simulation **1** was performed for 20 ns, and all the others for 50 ns. Coordinates were output at 0.2 ps intervals in simulations **1** through **4**, and 0.5 ps intervals in **5** and **6**.

### 3.2. Analysis of simulations

Analysis of hydrogen-bonds and water structure was performed in the following way. As used previously[20] a hydrogen-bonds was defined to exist when the donor H to acceptor O distance was less than 0.35 nm and the angle OH to O was less than 60° from linear. Hydrogen-bonds were calculated for every frame in each simulation, and the average occupancy calculated for each interaction; those with a frequency less than 2% were discarded. Hydrogen-bonds involving water-bridges were calculated in the same way. A water-bridge was counted when a water molecule was hydrogen-bonded to more than two distinct polar groups. All possibilities of donor/acceptor were considered the same, and again the percentage occupancy was calculated for each simulation. Any water bridges with a frequency less than 10% were discarded.

The conformation at glycosidic linkages was described by the notation used in the NMR literature, rather than that of IUPAC. This uses the hydrogen atoms as a basis; thus $\phi \equiv$ H1–C1–O*x*–C*x* and $\psi \equiv$ C1–O*x*–C*x*–H*x*. At (1→6) linkages the major conformers are defined using the standard chemistry notation *gg*, *gt*, and *tg*, which have been described previously.[14]

## Acknowledgements

Funding for this research was provided by both the Wellcome Trust, UK, and the Biotechnology and Biological Sciences Research Council, UK.

## References

1. Varki, A. *Glycobiology* **1993**, *3*, 97–130.
2. Dwek, R. A. *Chem. Rev.* **1996**, *96*, 683–720.
3. Imberty, A.; Pérez, S. *Chem. Rev.* **2000**, *100*, 4567–4588.

4. Duus, J. Ø.; Gotfredsen, C. H.; Bock, K. *Chem. Rev.* **2000**, *100*, 4589–4614.
5. Kirschner, K. N.; Woods, R. J. *Proc. Natl. Acad. Sci. U.S.A.* **2001**, *98*, 10541–10545.
6. Liu, Q.; Brady, J. W. *J. Phys. Chem. B* **1997**, *101*, 1317–1321.
7. Liu, Q.; Schmidt, R. K.; Teo, B.; Karplus, P. A.; Brady, J. W. *J. Am. Chem. Soc.* **1997**, *119*, 7851–7862.
8. Leroux, B.; Bizot, H.; Brady, J. W.; Tran, V. *Chem. Phys.* **1997**, *216*, 349–363.
9. Schmidt, R. K.; Karplus, M.; Brady, J. W. *J. Am. Chem. Soc.* **1996**, *118*, 541–546.
10. Liu, Q.; Brady, J. W. *J. Am. Chem. Soc.* **1996**, *118*, 12276–12286.
11. Brady, J. W. *J. Am. Chem. Soc.* **1989**, *111*, 5155–5165.
12. Almond, A.; Sheehan, J. K. *Glycobiology* **2003**, *13*, 255–264.
13. Almond, A.; Petersen, B. O.; Duus, J. Ø. *Biochemistry* **2004**, *43*, 5853–5863.
14. Almond, A.; Duus, J. Ø. *J. Biomol. NMR* **2001**, *20*, 351–363.
15. Almond, A.; Bunkenborg, J.; Franch, T.; Gotfredsen, C. H.; Duus, J. Ø. *J. Am. Chem. Soc.* **2001**, *123*, 4792–4802.
16. Almond, A.; Sheehan, J. K. *Glycobiology* **2000**, *10*, 329–338.
17. Almond, A.; Brass, A.; Sheehan, J. K. *J. Mol. Biol.* **1998**, *284*, 1425–1437.
18. Almond, A.; Brass, A.; Sheehan, J. K. *J. Phys. Chem. B* **2000**, *104*, 5634–5640.
19. Jorgensen, W. L.; Chandrasekhar, J.; Madura, J. D.; Impey, R. W.; Klein, M. L. *J. Chem. Phys.* **1983**, *79*, 926–935.
20. Brady, J. W.; Schmidt, R. K. *J. Phys. Chem.* **1993**, *97*, 958–966.
21. Almond, A.; Sheehan, J. K.; Brass, A. *Glycobiology* **1997**, *7*, 597–604.
22. Lis, H.; Sharon, N. *Eur. J. Biochem.* **1993**, *218*, 1–27.
23. Naidoo, K. J.; Brady, J. W. *J. Am. Chem. Soc.* **1999**, *121*, 2244–2252.
24. Brisson, J. R.; Carver, J. P. *Biochemistry* **1983**, *22*, 3680–3686.
25. Ware, F. E.; Vassilakos, A.; Peterson, P. A.; Jackson, M. R.; Lehrman, M. A.; Williams, D. B. *J. Biol. Chem.* **1995**, *270*, 4697–4704.
26. Woods, R. J.; Pathiaseril, A.; Wormald, M. R.; Edge, C. J.; Dwek, R. A. *Eur. J. Biochem.* **1998**, *258*, 372–386.
27. Wormald, M. R.; Petrescu, A. J.; Pao, Y. L.; Glithero, A.; Elliott, T.; Dwek, R. A. *Chem. Rev.* **2002**, *102*, 371–386.
28. Sayers, E. W.; Prestegard, J. H. *Biophys. J.* **2000**, *79*, 3313–3329.
29. Rutherford, T. J.; Neville, D. C. A.; Homans, S. W. *Biochemistry* **1995**, *34*, 14131–14137.
30. Rutherford, T. J.; Homans, S. W. *Biochemistry* **1994**, *33*, 9606–9614.
31. Balaji, P. V.; Qasba, P. K.; Rao, V. S. R. *Glycobiology* **1994**, *4*, 497–515.
32. Petrescu, A. J.; Butters, T. D.; Reinkensmeier, G.; Petrescu, S.; Platt, F. M.; Dwek, R. A.; Wormald, M. R. *EMBO J.* **1997**, *16*, 4302–4310.
33. Becker, D. J.; Lowe, J. B. *Glycobiology* **2003**, *13*, 41R–53R.
34. Weimar, T.; Peters, T.; Pérez, S.; Imberty, A. *Theochem—J. Mol. Struct.* **1997**, *395*, 297–311.
35. Bush, C. A.; Yan, Z. Y. *Biophys. J.* **1988**, *53*, A101–A101.
36. Cagas, P.; Bush, C. A. *Biopolymers* **1990**, *30*, 1123–1138.
37. Mukhopadhyay, C.; Bush, C. A. *Biopolymers* **1991**, *31*, 1737–1746.
38. Yan, Z. Y.; Bush, C. A. *Biopolymers* **1990**, *29*, 799–811.
39. Chaturvedi, P.; Warren, C. D.; Altaye, M.; Morrow, A. L.; Ruiz-Palacios, G.; Pickering, L. K.; Newburg, D. S. *Glycobiology* **2001**, *11*, 365–372.
40. Martin-Pastor, M.; Bush, C. A. *Biochemistry* **2000**, *39*, 4674–4683.
41. Widmalm, G.; Venable, R. M. *Biopolymers* **1994**, *34*, 1079–1088.
42. Ishizuka, Y.; Nemoto, T.; Fujiwara, M.; Fujita, K.; Nakanishi, H. *J. Carbohydr. Chem.* **1999**, *18*, 523–533.
43. Day, A. J.; Sheehan, J. K. *Curr. Opin. Struct. Biol.* **2001**, *11*, 617–622.
44. Sugahara, K.; Mikami, T.; Uyama, T.; Mizuguchi, S.; Nomura, K.; Kitagawa, H. *Curr. Opin. Struct. Biol.* **2003**, *13*, 612–620.
45. Heatley, F.; Scott, J. E. *Biochem. J.* **1988**, *254*, 489–493.
46. Woods, R. J.; Dwek, R. A.; Edge, C. J.; Fraserreid, B. *J. Phys. Chem.* **1995**, *99*, 3832–3846.
47. Brooks, B. R.; Bruccoleri, R. E.; Olafson, B. D.; States, D. J.; Swaminathan, S.; Karplus, M. *J. Comput. Chem.* **1983**, *4*, 187–217.